Journal of Neuroscience Methods 185 (2010) 213–220

Contents lists available at ScienceDirect

Journal of Neuroscience Methods

journal homepage: www.elsevier.com/locate/jneumeth

Heterologous functional expression system for odorant receptors

Hiroshi Hamana[1], Li Shou-xin[2], Laure Breuils[3], Junzo Hirono, Takaaki Sato*

Research Institute for Cell Engineering, National Institute of Advanced Industrial Science and Technology, 3-11-46 Nakoji, Amagasaki, Hyogo 661-0974, Japan

ARTICLE INFO

Article history:
Received 10 July 2009
Received in revised form 30 August 2009
Accepted 22 September 2009

Keywords:
Odorant receptor
Heterologous functional expression
HEK293
Calcium imaging
Gα
RTP
OR-S6

ABSTRACT

Heterologous functional expression system for odorant receptors (ORs) is essential for investigating the structure–activity relationship (SAR) of various ligands. Different systems that coexpressed ORs with different G-protein α subunits (Gα) demonstrated inconsistent effects on weak agonists and antagonists, but retained original relative sensitivities to potent agonists. In order to maintain the binding specificity of Gα to ORs, we constructed a chimeric $G\alpha_{15\text{-}olf}$, which contained the $G\alpha_{15}$ sequence with the conserved C-terminal region of $G\alpha_{olf}$. The Ca^{2+} responses of the HEK293 cells that coexpressed OR-S6 with $G\alpha_{15\text{-}olf}$ were more robust and reproducible compared to those of cells that coexpressed OR-S6 with $G\alpha_{15}$. Furthermore, $G\alpha_{15}$ sometimes induced unstable Ca^{2+} responses that limited the accuracy of quantitative comparison of peak responses. Our results showed that a heterologous expression system that coexpressed ORs with $G\alpha_{15\text{-}olf}$ and receptor transporting proteins was suitable for SAR analysis of various ligands.

1. Introduction

In mice, approximately 1000 different odorant receptors (ORs), which belong to G-protein-coupled receptors (GPCRs), discriminate and detect a subset of odorants in the respective olfactory sensory neurons (OSNs) (Buck and Axel, 1991; Sato et al., 1994; Malnic et al., 1999; Mori et al., 1999; Touhara et al., 1999; Zhang and Firestein, 2002; Hamana et al., 2003; Araneda et al., 2004). To elucidate the molecular basis of odor discrimination mechanism, it is necessary to determine the odorant specificity of each OR; it is examined by determining the structure–activity relationship (SAR) of various ligands for a target OR. At present, the detailed odorant specificities of ORs have been mostly unknown, partly because of the experimental difficulty in identifying responses of identical ORs from an average OSN subpopulation of as low as 0.1%.

The discovery of the receptor transporting proteins (RTPs) enabled the heterologous functional expression of many ORs (Saito et al., 2004). However, some of different systems that coexpressed different α subunits of G-proteins (Gα) demonstrated inconsistent effects on weak agonists and antagonists and showed similar relative sensitivities to potent agonists (Krautwurst et al., 1998; Floriano et al., 2000; Kajiya et al., 2001; Saito et al., 2004; Katada et al., 2005; Shirokova et al., 2005; Abaffy et al., 2006, 2007; Zhuang and Matsunami, 2007). OR-S6 that was specifically sensitive to nonanedioic acid (cc9) and possessed the charged amino acid residues at the conserved positions (Malnic et al., 1999) was classified into class-I OR (Zhang and Firestein, 2002). Octanoic acid (mc8) was reported as an agonist for OR-S6 in HeLa/15 cells that coexpressed $G\alpha_{15}$, while it was shown to be an antagonist of the same OR in HeLa/Olf cells that coexpressed $G\alpha_{olf}$ (Shirokova et al., 2005). In order to conduct a detailed SAR analysis of several series of ligands in heterologous functional expression systems, we considered the structure of Gα.

In the OSNs, odorant signals activate ORs and are transfered to $G\alpha_{olf}$ and amplified by 2 subsequent processes. First, the signal is amplified by the cyclic adenosine 3′,5′-monophosphate (cAMP) 2nd messenger system via $G\alpha_{olf}$-dependent adenylyl cyclase and resulted in generation of receptor potential by inward currents through cAMP-gated channels (Lancet, 1986; Nakamura and Gold, 1987; Jones and Reed, 1989; Bakalyar and Reed, 1990; Gold, 1999; Takeuchi and Kurahashi, 2005). Second, the inward Cl^- currents through Ca^{2+}-dependent Cl^- channels, which is activated by intracellular Ca^{2+} passed through cAMP-gated channels, amplifies the receptor potential in a nonlinear manner (Kleene, 1993; Kurahashi and Yau, 1993; Lowe and Gold, 1993). Subsequently, the receptor potential causes a transient Ca^{2+} increase via Ca^{2+} influx through voltage-dependent Ca^{2+} channels (Sato et al., 1991; Sato, 1994; Zufall et al., 2000). Because OSNs endogenously contain all the signal cascade components required for signal amplifications and cause a transient increase in Ca^{2+} levels, isolated OSNs are ideal for measuring relative sensitivities of a particular OR by Ca-imaging

* Corresponding author. Tel.: +81 6 6494 7816; fax: +81 6 6494 7861.
E-mail address: taka-sato@aist.go.jp (T. Sato).
[1] Present address: Department of Bioengineering and Robotics, Graduate School of Engineering, Tohoku University, Sendai, Miyagi 980-8579, Japan.
[2] Present address: Tongji Hospital, Tongji Medical College, Huazhong University of Science and Technology, Wuhan 430030, China.
[3] Present address: Tecnoscent, 1070 Brussels, Belgium.

0165-0270/$ – see front matter © 2009 Elsevier B.V. All rights reserved.
doi:10.1016/j.jneumeth.2009.09.024

(Hirono et al., 1992; Sato et al., 1994; Malnic et al., 1999; Touhara et al., 1999; Hamana et al., 2003). However, isolated OSNs show a gradual decrease in odor responsiveness, because of apoptosis induction due to cutting the axons during isolation (Carson et al., 2005). Thus, it is necessary to develop a functional expression system to elucidate the detailed SRA analysis of several series of ligands for a target OR. Notably, $G\alpha_{15}$ was used to drive the OR-induced Ca^{2+} increases via the activation of the inositol 1,4,5-trisphosphate (IP_3) signaling cascade because of its low specificity for GPCRs (Kajiya et al., 2001; Katada et al., 2005; Shirokova et al., 2005; Touhara, 2007).

In this study, we used a transient expression in HEK293 cells (Krautwurst et al., 1998; Kajiya et al., 2001) and investigated the effects of different Gα on odorant responsiveness of a few ORs by determining the differences in cellular Ca^{2+} responses. In order to maintain the binding specificity of Gα to ORs, we constructed a chimeric $G\alpha_{15\_olf}$, which mostly contained $G\alpha_{15}$ sequences (Kajiya et al., 2001) along with the conserved the C-terminal region of $G\alpha_{olf}$ (Jones and Reed, 1989). The HEK293 cells that coexpressed OR-S6 with $G\alpha_{15\_olf}$ demonstrated more rapid and robust responses to odorants compared to those that coexpressed OR-S6 with $G\alpha_{15}$. Furthermore, $G\alpha_{15}$-expressing cells sometimes showed unstable Ca^{2+} responses that limited the accuracy of quantitative comparison of response amplitudes. Our results showed that a heterologous expression system that coexpresses RTPs and $G\alpha_{15\_olf}$ was suitable for determining the detailed odorant specificities of target ORs.

2. Materials and methods

2.1. Odorants

All odorants of the available purest grades were commercially purchased. Heptanol (mh7), octanol (mh8), nonanol (mh9), decanol (mh10), heptanoic acid (mc7), mc8, nonanoic acid (mc9), decanoic acid (mc10), and dodecanoic acid (mc12) were purchased from Fluka through Sigma-Aldrich (St. Louis, MO, USA); undecanoic acid (mc11), decanedioic acid (cc10), 8-bromooctanoic acid (bc8), (R)-(−)-carvone (R-car), and (S)-(+)-carvone (S-car) from Sigma-Aldrich; heptanedioic acid (cc7), octanedioic acid (cc8), and cc9 from Wako Chemical Co. (Osaka, Japan); 7-bromoheptanoic acid (bc7) and 9-bromononanoic acid (bc9) from Matrix Scientific Inc. (Colombia, SC, USA). Odorants were dissolved in imaging buffer (140 mM NaCl, 5 mM KCl, 1.8 mM $CaCl_2$, 1.2 mM $MgSO_4$, 10 mM HEPES, 10 mM glucose, 1.2 mM KH_2PO_4, pH 7.2).

2.2. Construction of expression vectors

A synthetic DNA encoding the first 20 amino acid residues of human rhodopsin (MNGTEGPNFYVPFSNATGVV), which included HindIII and EcoRI recognition sequence at the 5′- and 3′-end, respectively, was introduced into the multiple cloning sites of *ph*CMV1 vector (Genlantic Inc., San Diego, CA, USA). This vector (Rho-tag/*ph*CMV1) was used for the expression of the rhodopsin-tagged OR. The coding sequence of the OR-S6 was amplified from mouse genomic DNA by polymerase chain reaction (PCR) and cloned into the EcoRI/BamHI sites of Rho-tag/*ph*CMV1. The other OR expression vectors were constructed in the same manner. The coding sequences of *RTP1* and *RTP2* were amplified from mouse brain poly (A)+RNA by reverse transcription (RT)-PCR and cloned into the EcoRI/KpnI and HindIII/BamHI sites of *ph*CMV1, respectively. Chimeric $G\alpha_{15\_olf}$ was designed in such a way that the C-terminal region of G_{olf} α subunit, which was a determinant of binding specificity of Gα to GPCRs (Conklin et al., 1996; Saito et al., 1999), was conserved. To construct the $G\alpha_{15\_olf}$ expression vector, we amplified $G\alpha_{15}$ cDNA by RT-PCR from mouse brain poly (A)+RNA and cloned into the BamHI/XbaI sites of *p*BK-CMV (Stratagene Ltd, Cambridge, UK) that has a deletion of NheI–SpeI fragment. The KpnI–XbaI fragment of $G\alpha_{15}$/*p*BK-CMV, which encodes the last 9 amino acids and stop codon of $G\alpha_{15}$, was replaced with the synthetic DNA. The resultant vector ($G\alpha_{15\_olf}$/*p*BK-CMV) could express the chimeric $G\alpha_{15\_olf}$, in which the last 7 amino acids (LDEINLL) of $G\alpha_{15}$ were replaced by the last 7 amino acids (LKQYELL) of rat $G\alpha_{olf}$.

2.3. Heterologous functional expression of ORs in HEK293 cells

HEK293 cells (human embryonal kidney 293 cells, JCRB9068) were purchased from the Japanese Cancer Research Resource Bank (JCRB) Cell Bank through the Health Science Research Resource Bank (Osaka, Japan). The HEK293 cells were cultured and allowed to proliferate, following which they were frozen with freezing medium containing 90% heat-inactivated fetal bovine serum (FBS) and 10% dimethyl sulfoxide in stock tubes at −80 °C, and stored in liquid N_2. OR-S6, OR-S83 (Malnic et al., 1999), OR-car-c5 (MOR130-2), OR-car-n266 (MOR202-37), or OR-car-n270 (MOR186-2) (Zhang and Firestein, 2002; Hamana et al., 2003) was expressed in HEK293 cells (Krautwurst et al., 1998) along with RTP1, RTP2 (Saito et al., 2004), and $G\alpha_{15}$ (Kajiya et al., 2001) or $G\alpha_{15\_olf}$. HEK293 cells were grown in culture dishes containing Dulbecco's modified essential medium (D-MEM) with 10% FBS without antibiotics at 37 °C under a humidified atmosphere containing 5% CO_2 and were passaged every 2 or 3 days before the cells reached confluency. Confluent cells (60–80%) cultured in poly-D-lysine-coated glass-bottomed 35-mm dishes (MatTek Co., Ashland, MA, USA) were transfected with 2.0 μg Rho-OR/*ph*CNV1, 0.5 μg RTP1/*ph*CMV1, 0.5 μg RTP2/*ph*CMV1 and 1.0 μg $G\alpha_{15\_olf}$/*p*BK-CMV (or $G\alpha_{15}$/*p*BK-CMV) by using 8 μl lipofectamin 2000 (Invitrogen, Carlsbad, CA, USA), according to manufacturer's instructions.

2.4. Ca-imaging of cellular responses of HEK293 cells

Cellular Ca^{2+} responses of OR-S6 were measured by single-cell fura-2 fluorescence ratio imaging. The transfected cells were cultured for 24–28 h and incubated with 5 μM fura-2/AM (Molecular Probe, Eugen, OR, USA) for 30 min at 37 °C. The dye solution was replaced with imaging buffer, and cells were placed in the dark for 30 min at room temperature before initiating Ca-imaging. During Ca-imaging, the bath solution within the culture dish was limited to a volume of approximately 50 μl by setting a recording adaptor with a glass slip ceiling. Odorant solutions were applied to the cells using a peristaltic pump at a flow rate of 1.5 ml/min for 20 s. Cells were observed under an epifluorescence microscopy (TE2000; Nikon, Kanagawa, Japan), alternatively excited at 340 nm or 380 nm, and the 510-nm fluorescence images (F_{340} and F_{380}) were sequentially recorded using a Ca-imaging system (AQUACOSMOS; Hamamatsu Photonics Co., Shizuoka, Japan). Ca^{2+} responses were compared with respect to the peak fluorescence ratios of F_{340}/F_{380}.

2.5. Data analysis

In order to calculate onset latency of Ca^{2+} response, peak width at half-maximum, and time constant of exponential decay, increase in the levels of Ca^{2+} from the onset of the response to approximately 90% of the peak value was fitted by a single-exponential function, and Ca^{2+} recovery around half-maximum was also fitted by a single-exponential function by using Microsoft Office Excel 2003 (Microsoft Corp., USA). Onset latency was calculated as the time from the onset of the stimulus to the increase in Ca^{2+} levels that were equivalent to the sum of the SD value and the average baseline value. Dose–response curve was fitted with a logistic function by using the OriginPro (ver. 7; OriginLab Corp., Northampton, MA, USA). All the values have been represented as mean ± standard

error (S.E.). All the differences between parameters were evaluated by one-way ANOVA in the OriginPro.

3. Results

3.1. Coexpression of RTPs increased the number of responsive HEK293 cells that expressed ORs

First, we confirmed whether the RTPs facilitated the functional expression of the ORs in HEK293 cells, as has been reported in HEK293T cells (Saito et al., 2004). OR-S6 and $G\alpha_{15}$ were expressed with or without RTPs in HEK263 cells. When the transfected cells were stimulated by 10 μM cc9, the frequency of responsive cells that coexpressed OR-S6 with RTPs and $G\alpha_{15}$ increased to 5.9% (40/680), which was about 8 times that of the responsive cells coexpressing only $G\alpha_{15}$ (0.7%, 4/540). However, the response amplitudes of cells coexpressing OR-S6 with RTPs and $G\alpha_{15}$ were similar to those of cells coexpressing OR-S6 with $G\alpha_{15}$ alone (Fig. 1a and b). Average peak response amplitudes of the cells coexpressing OR-S6 with RTPs and $G\alpha_{15}$ remained constant at cc9 concentrations of 10–1000 μM. These values normalized by those of 1 mM response amplitudes were 0.96 ± 0.06 ($n = 40$) and 0.95 ± 0.04 at concentrations of 10 and 100 μM, respectively. Hence, in order to improve odorant responsiveness of the functional expression system by enhancing the binding specificity of Gα to ORs, we constructed a chimeric $G\alpha_{15\_olf}$. It was expected that the facilitation in the binding specificity of Gα to ORs would improve the efficiency of the functional expression system by enabling it to produce rapid and robust responses and to be sensitive to detect small differences in OR responses to weak agonists or antagonists.

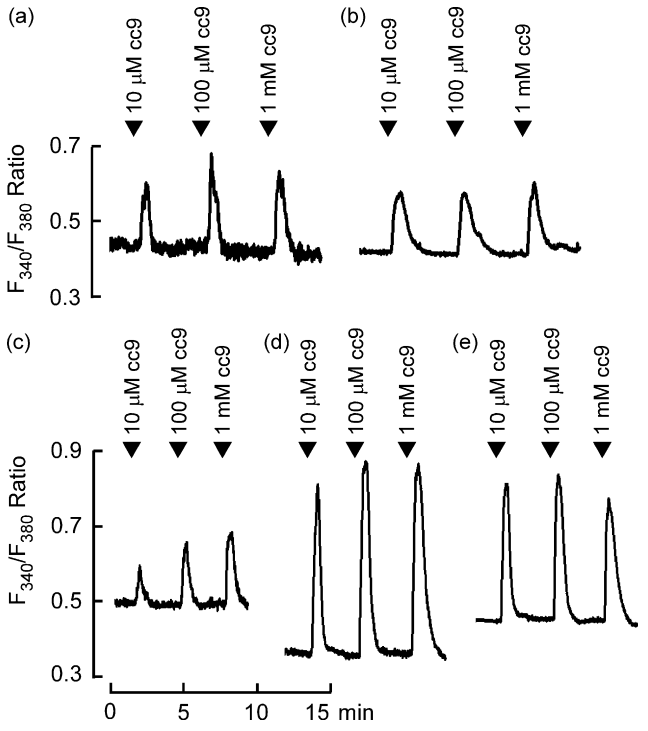

Fig. 1. $G\alpha_{15\_olf}$ mediated more rapid and robust OR-S6 responses compared to $G\alpha_{15}$. (a–e) Responses of OR-S6 to nonanedioic acid (cc9) in HEK293 cells that coexpressed $G\alpha_{15}$ (a), $G\alpha_{15}$ + RTP1 + RTP2 (b), $G\alpha_{15\_olf}$ (c), $G\alpha_{15\_olf}$ + RTP1 + RTP2 (d), and $G\alpha_{15\_olf}$ + RTP1 (e). Responses of cells coexpressing OR-S6 with $G\alpha_{15\_olf}$ showed more rapid and robust changes compared to those of cells coexpressing OR-S6 with $G\alpha_{15}$. Average Ca^{2+} response curves are represented as fura-2 fluorescence ratios of F_{340}/F_{380} for 4 (a), 40 (b), 4 (c), 17 (d), and 30 (e) sensitive cells out of the 260–680 cells tested. Odorants were applied to the HEK293 cells for 20 s at the times indicated by the arrowheads.

3.2. The chimeric $G\alpha_{15\_olf}$ mediated more robust Ca^{2+} responses of OR-S6 than $G\alpha_{15}$

The chimeric $G\alpha_{15\_olf}$ was mainly $G\alpha_{15}$ (Kajiya et al., 2001) containing the conserved C-terminal region of $G\alpha_{olf}$ (Jones and Reed, 1989), which was considered as the binding site for GPCRs (Conklin et al., 1996; Saito et al., 1999). At 10 μM of cc9, cells coexpressing OR-S6 with RTPs and $G\alpha_{15\_olf}$ also showed an increased responsive cell rate (5.7%, 17/300) that was about 6 times that of the cells coexpressing $G\alpha_{15\_olf}$ alone (1%, 4/400) (Fig. 1c and d).

Furthermore, in HEK293 cells, the chimeric $G\alpha_{15\_olf}$ mediated > twofold greater Ca^{2+} responses of OR-S6 than $G\alpha_{15}$ (Fig. 1b and d, Table 1). Among the tested combinations of coexpressed components, the combination of RTP1, RTP2, and $G\alpha_{15\_olf}$ mediated OR-S6 to elicit the greatest Ca^{2+} responses in HEK293 cells. Average peak response amplitudes of the cells that coexpressed OR-S6 with RTPs and $G\alpha_{15\_olf}$ decreased slightly with decreasing cc9 concentration: at cc9 concentration of 100 μM, the response amplitude was 1.00 ± 0.03 (normalized by that of 1 mM response amplitude, $n = 17$), while at cc9 concentration of 10 μM, the response amplitude decreased to 0.88 ± 0.05 ($n = 17$). On the other hand, average peak response amplitudes of the cells that coexpressed OR-S6 with $G\alpha_{15\_olf}$ alone clearly decreased to 0.82 ± 0.01 ($n = 4$) and 0.55 ± 0.04 at cc9 concentrations of 100 μM and 10 μM, respectively. Cells coexpressing OR-S6 with $G\alpha_{15\_olf}$ and RTP1 alone also showed higher responsive cell rate (12%, 30/260), which was about 12 times that of cells coexpressing only $G\alpha_{15\_olf}$ (1%, 4/400) (Fig. 1c and e).

Regarding the response kinetics, $G\alpha_{15\_olf}$ mediated more rapid increase and recovery of Ca^{2+} responses than $G\alpha_{15}$. Onset latencies of Ca^{2+} responses for $G\alpha_{15\_olf}$ were shorter by about 0.9, 0.5, and 0.5 times than those of $G\alpha_{15}$ at cc9 concentrations of 10, 100, and 1000 μM, respectively. The respective onset latencies of the OR-S6 responses for $G\alpha_{15\_olf}$ were 23.0 ± 8.4 s ($n = 17$), 12.5 ± 7.9 s, 10.6 ± 6.8 s, whereas those for $G\alpha_{15}$ were 26.0 ± 11.9 s ($n = 40$), 25.0 ± 9.2 s, 22.4 ± 9.6 s (Table 1). Average latencies of peak responses and/or their SDs were greater for $G\alpha_{15}$ than for $G\alpha_{15\_olf}$. This greater variation in peak latencies was consistent with the greater difference between the peak amplitude of an average response curve (Fig. 1b and d) and the average peak response amplitude of 40 cells for $G\alpha_{15}$ (latter/former = 151–165%) at each odorant concentration compared to that of 17 cells for $G\alpha_{15\_olf}$ (latter/former = 115–118%) (Table 1). In the case of $G\alpha_{15\_olf}$, increased peak width at half-maximum of Ca^{2+} response was attributable to increased stimulus intensity (Fig. 2a and b). However, peak widths at half-maximum for $G\alpha_{15}$ showed inconsistent changes with increased stimulus intensity.

Especially, peak response amplitudes and time constants of single-exponential decays of OR-S6 responses indicated remarkable differences between $G\alpha_{15\_olf}$ and $G\alpha_{15}$ (Figs. 1b,d and 2b, Table 1). At 100 μM of cc9, relatively large SDs for peak width at half-maximum and decay time constant suggested greater variations in the cellular responses for $G\alpha_{15}$ than for $G\alpha_{15\_olf}$. Except for 3 cases, all kinetic parameters for the OR-S6 responses were significantly different between $G\alpha_{15\_olf}$ and $G\alpha_{15}$ ($P < 0.05$; Table 1). The kinetic parameters of the OR-S83 responses were also significantly different between $G\alpha_{15\_olf}$ and $G\alpha_{15}$ (Supplementary Table S1). Notably, of the 40 responsive cells that coexpressed OR-S6 with RTPs and $G\alpha_{15}$, 20 (50%) demonstrated unstable Ca^{2+} responses (as shown in Fig. 3c and c′ insert). On the other hand, none of 17 responsive cells that coexpressed OR-S6 with RTPs and $G\alpha_{15\_olf}$ demonstrated such unstable responses. These response fluctuations limited the accuracy of performing quantitative comparison of peak response amplitudes. Thus, coexpression of RTPs and $G\alpha_{15\_olf}$ improved responsiveness of OR-S6, with respect to response amplitudes and kinetics, compared to the coexpression of RTPs and $G\alpha_{15}$.

Table 1
Differences in OR-S6 response kinetics between $G\alpha_{15\_olf}$ and $G\alpha_{15}$.

Agonist	$G\alpha_{15\_olf}$	$G\alpha_{15}$	Significance
Onset latency of Ca^{2+} response			
10 μM cc9	23.0 ± 2.0	26.0 ± 1.8	$P = 0.34755$
100 μM cc9	12.5 ± 1.9	25.0 ± 1.5	$P = 0.00001$
1 mM cc9	10.6 ± 1.7	22.4 ± 1.5	$P = 0.00003$
Latency of peak response			
10 μM cc9	38.4 ± 1.3	39.0 ± 2.3	$P = 0.87573$
100 μM cc9	28.3 ± 1.5	38.4 ± 1.9	$P = 0.00154$
1 mM cc9	25.5 ± 2.3	34.3 ± 1.7	$P = 0.05850$
Peak response amplitude			
10 μM cc9 (%Average response)	0.52 ± 0.05 (116% of 0.449)	0.25 ± 0.02 (155% of 0.164)	$P < 0.00001$
100 μM cc9 (%Average response)	0.60 ± 0.06 (115% of 0.518)	0.26 ± 0.02 (165% of 0.156)	$P < 0.00001$
1 mM cc9 (%Average response)	0.60 ± 0.05 (118% of 0.504)	0.28 ± 0.02 (151% of 0.185)	$P < 0.00001$
Peak width at half-maximum			
10 μM cc9	22.0 ± 2.0	38.7 ± 3.1	$P = 0.00159$
100 μM cc9	31.2 ± 2.2	37.8 ± 3.8	$P = 0.00159$
1 mM cc9	37.9 ± 2.4	26.3 ± 1.7	$P = 0.00037$
Time constant of single-exponential decay for Ca^{2+} recovery			
10 μM cc9	36.4 ± 2.2	179 ± 21	$P = 0.00004$
100 μM cc9	40.2 ± 3.5	240 ± 30	$P = 0.00005$
1 mM cc9	66.7 ± 10.1	170 ± 22	$P = 0.00459$

Parameters for Ca^{2+} responses of OR-S6 in HEK293 cells are shown as mean ± S.E. Peak response amplitude is shown as an average of peak response amplitudes and the ratio (%) to the average response is shown in parentheses. An average was calculated for $G\alpha_{15\_olf}$ ($n = 17$) and $G\alpha_{15}$ ($n = 40$). Except for 3 cases, all parameters were significantly different between $G\alpha_{15\_olf}$ and $G\alpha_{15}$ ($P < 0.05$, one-way ANOVA).

3.3. *$G\alpha_{15\_olf}$ improved the performance of the expression system while being sensitive to small differences in Ca^{2+} responses*

Next, we compared the performance of the OR expression system coexpressing RTPs and $G\alpha_{15\_olf}$ with that of the OR expression system coexpressing RTPs and $G\alpha_{15}$ with reference to the ability to discriminate small differences in Ca^{2+} responses. In HeLa/Olf cells, the 50% effective concentration (EC_{50}) of cc9 was 0.7 ± 0.06 μM and mc8 was found to be a weak antagonist for OR-S6 (Shirokova et al., 2005). Using approximately 50-fold higher concentration of cc9 than the EC_{50}, we compared the inhibitory effect of the antagonist

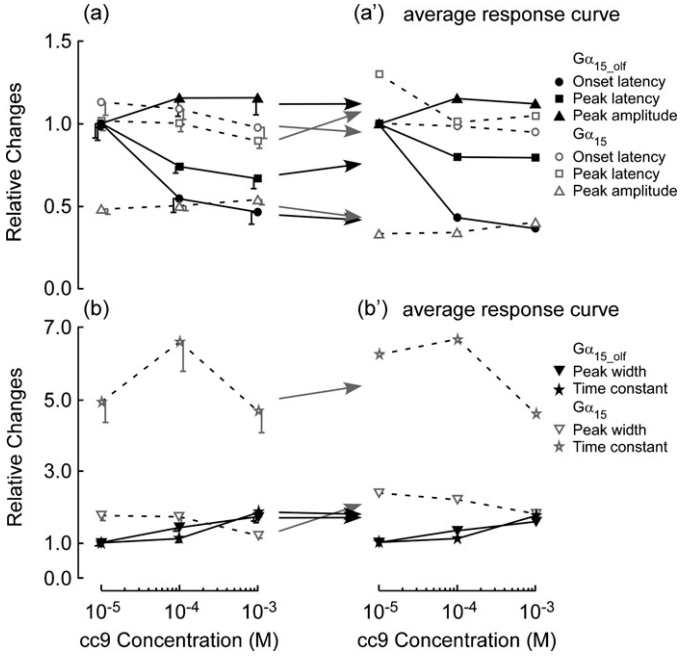

Fig. 2. Differences in dose-dependent changes in Ca^{2+} response kinetics. (a) Onset latency, time taken to elicit the response peak, and response peak amplitude for cells coexpressing OR-S6 with $G\alpha_{15\_olf}$ + RTP1 + RTP2 ($n = 17$) or for those coexpressing OR-S6 with $G\alpha_{15}$ + RTP1 + RTP2 ($n = 40$). (b) Half- and time constant of exponential decay. With increasing concentrations of cc9, there were systematic changes in the response parameters of the cells coexpressing OR-S6 and $G\alpha_{15\_olf}$, whereas such changes were not observed for those coexpressing OR-S6 and $G\alpha_{15}$. Each response parameter was normalized by the respective response maximum width parameter of the cells coexpressing OR-S6 and $G\alpha_{15\_olf}$ to 10 μM cc9.

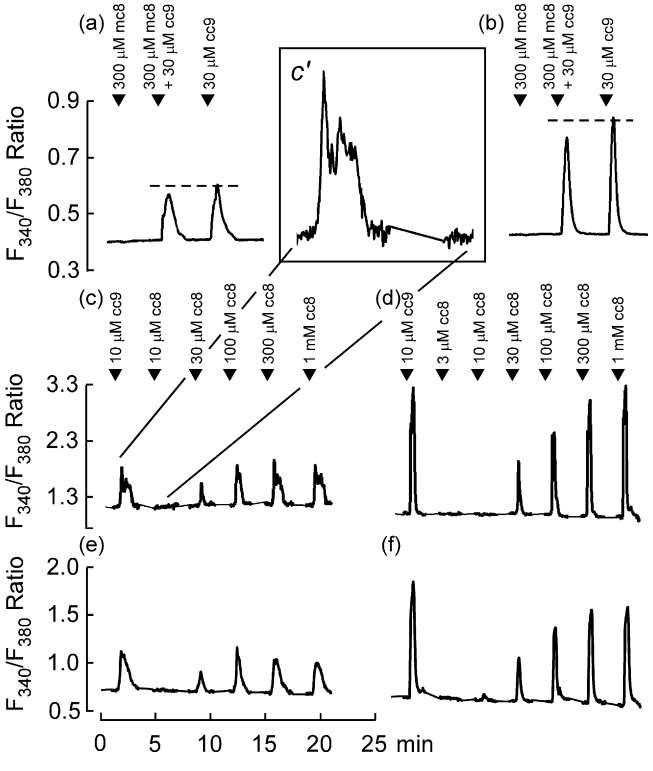

Fig. 3. Gα-dependent difference in Ca^{2+} responses of OR-S6. (a–f) Response of OR-S6 to cc9 and octanedioic acid (cc8) and the former weak inhibition by octanoic acid (mc8) in HEK293 cells that coexpressed OR-S6 with RTP1, RTP2, and $G\alpha_{15}$ (*a*, *c*, *e*) or $G\alpha_{15\_olf}$ (b, d, f). Responses of cells coexpressing OR-S6 with $G\alpha_{15\_olf}$ were greater in relative amplitudes and showed more rapid changes than those of cells coexpressing OR-S6 with $G\alpha_{15}$. Coexpression of $G\alpha_{15}$ sometimes induced unstable responses in amplitudes (c and c′ insert). Average Ca^{2+} responses for 35 (a), 83 (b), 16 (e), and 22 (f) cells or Ca^{2+} responses of single cells (c and d) are demonstrated.

mc8 on the OR-S6 response between the HEK293 cells coexpressing $G\alpha_{15\_olf}$ and those coexpressing $G\alpha_{15}$.

Difference between the peak amplitudes of an average response curve of OR-S6 to 30 μM cc9 and an average inhibitory response curve to a mixture of 30 μM cc9 and 300 μM mc8 was greater in the cells coexpressing $G\alpha_{15\_olf}$ (0.073) than in those coexpressing $G\alpha_{15}$ (0.037) (Fig. 3a and b). The response decrease in the average response curve for OR-S6 and $G\alpha_{15\_olf}$ was more close to the average response decrease of cells coexpressing OR-S6 with $G\alpha_{15\_olf}$ compared to that of $G\alpha_{15}$. In addition, there was less error in the average decrease in response amplitude for $G\alpha_{15\_olf}$ (0.074 ± 0.016; $n = 83$) than that for $G\alpha_{15}$ (0.073 ± 0.033; $n = 35$). Notably, although there was a significant difference in average response amplitude to mc8 + cc9 ($P = 0.0028$), as well as that of cc9 ($P = 0.00092$), between HEK293 cells coexpressing $G\alpha_{15}$ (0.30 ± 0.03; $n = 35$) and those coexpressing $G\alpha_{15\_olf}$ (0.43 ± 0.02, $n = 83$), the average ratio of the mc8 + cc9 response to the cc9 response for $G\alpha_{15}$ (0.86 ± 0.07; $n = 35$) was not significantly different from that of $G\alpha_{15\_olf}$ (0.87 ± 0.03, $n = 83$) ($P = 0.9644$). At least, the average response curve of HEK293 cells coexpressing OR-S6 with $G\alpha_{15\_olf}$ represented relative OR response amplitudes with small systemic errors than that of HEK293 cells coexpressing OR-S6 with $G\alpha_{15}$.

Further, we examined the differences in the responses of OR-S6 to a weak agonist, cc8 (Malnic et al., 1999; Zhuang and Matsunami, 2007). Coexpression of $G\alpha_{15\_olf}$ also reduced the systemic errors in the dose-dependent increase in OR-S6 responses to a weak agonist cc8. With an increase in the odorant concentration from 10 μM to 1 mM, there was a gradual increase in the Ca^{2+} responses of OR-S6 in the cells coexpressing $G\alpha_{15\_olf}$, but such an increase was not clearly observed at the concentrations of 300 μM and 1 mM in the cells coexpressing $G\alpha_{15}$ (Fig. 3c–f). Thus, coexpression of $G\alpha_{15\_olf}$ improved the performance of the HEK293 functional expression system while being sensitive to small differences in average Ca^{2+} response curves.

Dose response curves of OR-S6 for cc8 with respect to the Ca^{2+} responses of HEK293 cells coexpressing $G\alpha_{15\_olf}$ and RTPs and those coexpressing $G\alpha_{15}$ and RTPs are shown in Fig. 4. EC_{50} values of OR-S6 for cc8 was almost identical between cells coexpressing $G\alpha_{15\_olf}$ (25.8 ± 4.2 μM; $n = 22$) and those coexpressing $G\alpha_{15}$ (26.6 ± 2.4 μM; $n = 16$). However, the shapes of the dose response curves of cells for the both types of Gα slightly differed: the dose response curve of cells coexpressing OR-S6 and $G\alpha_{15\_olf}$ showed a moderate logistic fit compared to the steep dose response curve of cells coexpressing OR-S6 and $G\alpha_{15}$. In addition, at the concentration of 100 μM cc8, the relative response amplitudes of $G\alpha_{15\_olf}$ were significantly different from those of $G\alpha_{15}$ ($P = 0.02341$).

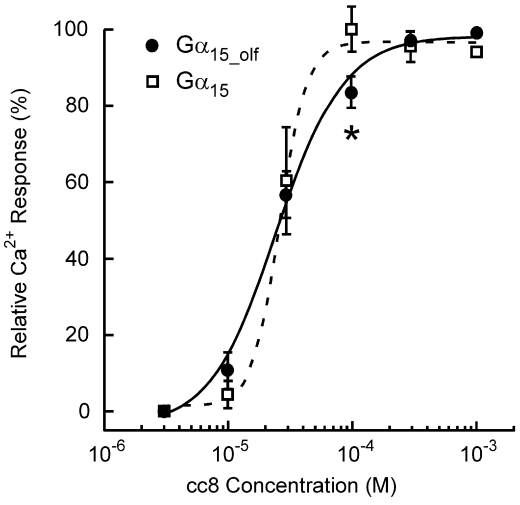

Fig. 4. The shapes of the dose response curves of OR-S6 were slightly different between $G\alpha_{15\_olf}$ and $G\alpha_{15}$. Dose response curves of OR-S6 for cc8 are shown with respect to the Ca^{2+} responses of HEK293 cells that coexpressed $G\alpha_{15\_olf}$ + RTP1 + RTP2 (closed circle) or those that coexpressed $G\alpha_{15}$ + RTP1 + RTP2 (open square). EC_{50} values of OR-S6 for cc8 were almost identical between cells coexpressing $G\alpha_{15\_olf}$ (25.8 ± 4.2 μM; mean ± S.E., $n = 22$) and those coexpressing $G\alpha_{15}$ (26.6 ± 2.4 μM; mean ± S.E., $n = 16$). However, the dose–response curve of OR-S6 + $G\alpha_{15\_olf}$ showed a moderate logistic fit compared to the steep dose–response curve of OR-S6 + $G\alpha_{15}$. In addition, at the concentration of 100 μM cc8, the relative response amplitudes of $G\alpha_{15\_olf}$ were significantly different from those of $G\alpha_{15}$ (marked by the asterisk). Ca^{2+} responses were compared with respect to peak fluorescence ratios normalized by the maximum response amplitudes.

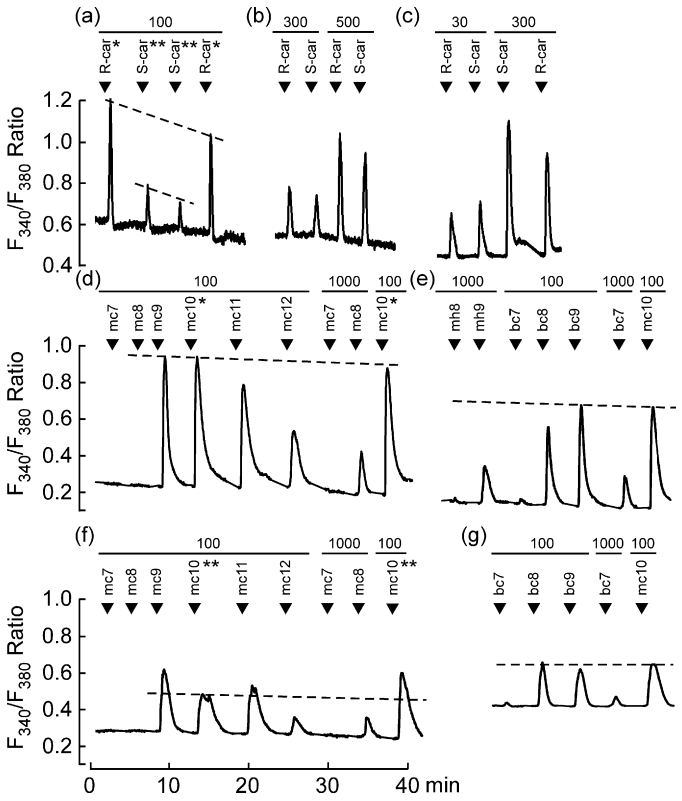

Fig. 5. Ca^{2+} responses of 4 ORs and difference between $G\alpha_{15\_olf}$ and $G\alpha_{15}$. (a–c) Average responses of OR-car-c5 (a), OR-car-n270 (b), OR-car-n266 (c) in HEK293 cells that coexpressed RTP1, RTP2, and $G\alpha_{15\_olf}$. (d–g) Average responses of OR-S83 in HEK293 cells that coexpressed RTP1, RTP2, and $G\alpha_{15\_olf}$ (d and e) or $G\alpha_{15}$ (f and g). Average responses of OR-car-c5 and OR-S83 in HEK293 cells that coexpressed $G\alpha_{15\_olf}$ (marked by a single or double asterisks in a and d) demonstrated good reproducibility with a constant decay rate, whereas those of cells that coexpressed $G\alpha_{15}$ (marked by double asterisks in f) were not identical even at the same concentration and changed more slowly with increasing time. Odorant concentrations are shown in μM.

3.4. $G\alpha_{15\_olf}$ mediated reproducible Ca^{2+} responses while retaining the original relative sensitivities of ORs

Finally, we confirmed whether the relative sensitivities of the 4 ORs were similar to those observed in the isolated OSNs and compared the response reproducibilities between the cells coexpressing $G\alpha_{15\_olf}$ and those coexpressing $G\alpha_{15}$. OR-car-c5 that had shown higher sensitivity to (R)-(−)-carvone (R-car) than to (S)-(+)-carvone (S-car) in the isolated OSNs (Hamana et al., 2003) also showed higher sensitivity to R-car than to S-car in the HEK293 cells (Fig. 5a). In addition, at an identical decay rate, higher and lower responses of OR-car-c5 in the cells that coexpressed $G\alpha_{15\_olf}$ were reproducibly observed (Fig. 5a, indicated by single or double asterisks). Moreover, OR-car-n270 and OR-car-n266 that had shown similar sensitivities to R- and S-car (Hamana et al., 2003) also showed similar sensitivities to both the carvones in the HEK293 cells (Fig. 5b and c).

OR-S83 was found to be highly sensitive to nonanoic acid (mc9) and nonanol (mh9) in the OSN (Malnic et al., 1999). Using the HEK293 cells coexpressing $G\alpha_{15\_olf}$ for the odorants that were not analyzed in the OSN, we found that OR-S83 responded to decanoic acid (mc10), undecanoic acid (mc11), dodecanoic acid (mc12), 9-bromononanoic acid (bc9), and 7-bromoheptanoic acid (bc7), as well as mc9. Our assay again showed good reproducibility for responses of OR-S83 (Fig. 5d, indicated by the asterisk). However, in the cells that coexpressed $G\alpha_{15}$, OR-S83 showed a significant difference in the peak response amplitudes to identical stimuli (Fig. 5f, indicated by the double asterisks). Except for the mh9 response that was relatively weaker than in the isolated OSN, the relative response amplitudes of HEK293 cells to fatty acids, aliphatic alcohols, and bromo-fatty acids were almost similar to those observed in the OSN (Fig. 5d and e).

At the tested concentrations, relative peak response amplitudes of OR-S83 in the cells that coexpressed $G\alpha_{15\_olf}$ seemed to be different from those of the cells coexpressing $G\alpha_{15}$ for the responses to mc9, mc10, mc11, 8-bromooctanoic acid (bc8), and bc9 (Fig. 5d–g). We thoroughly compared the cellular response kinetics and the consistency in the molecular-length dependencies between $G\alpha_{15\_olf}$ and $G\alpha_{15}$. This analysis revealed that response kinetics and average response curve of the heterologous expression system coexpressing $G\alpha_{15\_olf}$ better represented the structure activity relationship of homologous fatty acids for OR-S83 than that of coexpressing $G\alpha_{15}$.

3.5. *Response kinetics and average response curve for OR-S83 and $G\alpha_{15\_olf}$ indicate the contribution of the hydrophobic backbone of the ligand to the receptor–ligand interaction in a molecular-length dependent manner*

Because the OR-S83 responses to mono carboxylic acids were greater than those to dicarboxylic acids (Malnic et al., 1999), it can be speculated that OR-S83 activation requires hydrophobic interaction between OR-S83 and a hydrophobic region from a terminal methyl group to the backbone of the ligand contributes to ligand affinity to the receptor in a hydrocarbon-chain-length dependent manner. In our heterologous expression system, the OR-S83 responses and kinetic parameters also showed lesser variation for $G\alpha_{15\_olf}$ than for $G\alpha_{15}$ (Supplementary Table S1). Response rates to a given set of odorants varied among cells (Supplementary Figs. S1 and S2). In this study, we analyzed responses in the cells that showed 4/5 or higher response rates to responsive ligands.

In the Ca^{2+} responses that were shown in Fig. 5c–f, the molecular-length dependencies of response kinetics for the cells coexpressing OR-S83 and $G\alpha_{15\_olf}$ have been analyzed. Both the onset latencies and peak latencies were the lowest at the molecular length of 10 in the range of 8–12 carbon atoms (Fig. 6a and b). Kinetic parameters of average response curves were almost identical to those of the respective average parameters. At the ligand concentration of 100 μM, the response peak amplitudes showed the maximum values at the molecular length of 9 and 10 (Fig. 6c). This result suggests that ligand-binding pocket of OR-S83 is designed to accommodate 9- and 10-carbon-chain long ligands. The shorter latencies for mc10 than for mc9 could be attributable to a stronger hydrophobic interaction between the ligand backbone and OR-S83 ligand-binding pocket or a smaller conformational change during the ligand-binding-initiated OR-S83 activation in a molecular-length-dependent manner.

Both the peak width at half-maximum and time constants of single-exponential decay increased with increasing molecular length and hydrophobicity of the ligand in the tested range. This result suggests that a stronger hydrophobic interaction between OR-S83 and the ligand hydrocarbon chain elongates the ligand-binding time during receptor activation. However, the increase in onset latency and peak latency at the molecular lengths of 11 and

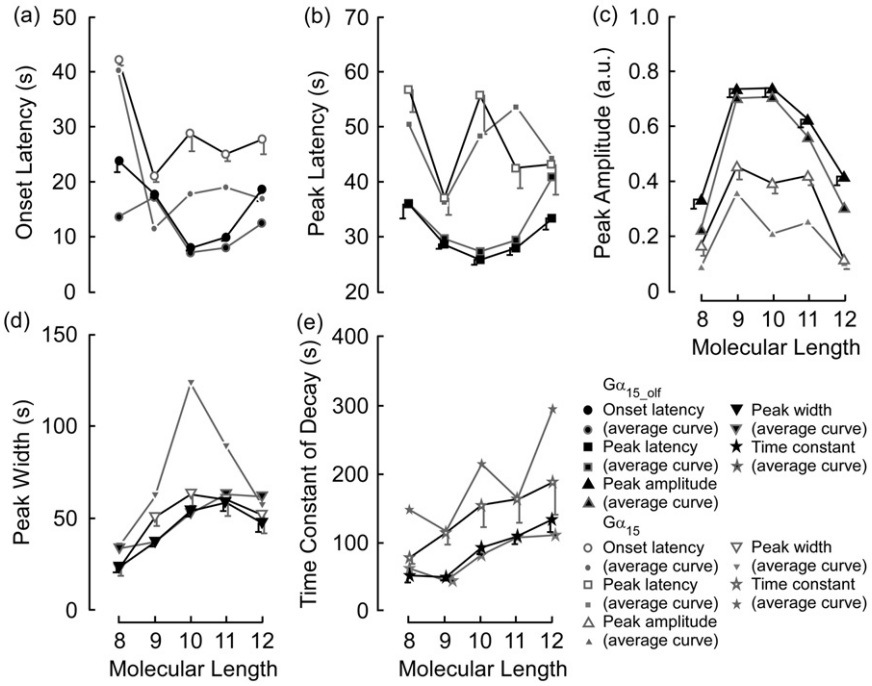

Fig. 6. Differences in molecular-length-dependencies in OR-S83 response kinetics. (a) Onset latency; (b) time taken to elicit the response peak; (c) response peak amplitude; (d) half-maximum width; and (e) time constant of exponential decay for cells coexpressing OR-S83 with $G\alpha_{15\_olf}$ + RTP1 + RTP2 (n = 29) or for those coexpressing OR-S83 with $G\alpha_{15}$ + RTP1 + RTP2 (n = 23). With increasing molecular lengths from 8 to 12 carbon atoms, there were systematic changes in the response parameters of the cells coexpressing OR-S83 and $G\alpha_{15\_olf}$, whereas such changes were not clearly observed for those coexpressing OR-S83 and $G\alpha_{15}$. Differences between the parameters of an average response curve and the average parameters (mean ± S.E.) of the cells coexpressing OR-S83 and $G\alpha_{15\_olf}$ were lesser than those coexpressing of OR-S83 and $G\alpha_{15}$. Fatty acids were used at the odorant concentration of 100 μM, except for octanoic acid (1 mM; molecular length = 8).

12 suggests that such stronger hydrophobic interactions do not contribute to the speed of OR-S83 activation.

In the case of $G\alpha_{15}$, the molecular-length dependencies of response kinetics became unclear. The onset latencies seemed to be the lowest at the molecular length of 9 (Fig. 6a). However, the minimum onset latency time was still longer than that for $G\alpha_{15\_olf}$ even in the range of 9–12. The peak latencies for $G\alpha_{15}$ demonstrated no clear molecular-length dependency (Fig. 6b). The peak amplitude for $G\alpha_{15}$ also showed a modified molecular-length dependency for $G\alpha_{15\_olf}$ (Fig. 6c). Compared to the other parameters, peak width and time constant of decay for $G\alpha_{15}$ were more similar to those for $G\alpha_{15\_olf}$, but the molecular-length dependencies were still unclear (Fig. 6d and e).

In addition, the peak amplitude of average OR-S6 response curve in the cells coexpressing $G\alpha_{15}$ was somewhat different from the order cc10 > cc8, which was observed in the cells coexpressing $G\alpha_{15\_olf}$ (Hamana et al., unpublished data) and in other systems (Abaffy et al., 2006; Zhuang and Matsunami, 2007) (Supplementary Fig. S3). Taken together, these results suggest that the ability of $G\alpha_{15\_olf}$ to mediate reproducible Ca^{2+} responses and maintain the original relative sensitivity of ORs was better than that of $G\alpha_{15}$. Moreover, our findings indicate that quantitative analyses of cells coexpressing ORs with $G\alpha_{15\_olf}$ are more reliable than those coexpressing ORs with $G\alpha_{15}$.

3.6. Cell passage number and other cell lines for functional OR expression system

During cell passaging, HEK293 cells showed a gradual change from a flat morphology to a round one. At <10 cell passages, HEK293 cells showed weak fura-2 fluorescence staining and rarely responded to agonists. Moreover, ORs did not respond to odorants in a dose-dependent manner in cells with high passage numbers; the reason for this is unclear. Hence, we performed Ca-imaging of HEK293 cells with passage numbers of 10–30 for ensuring uniformity in the results.

In the initial stage of this study, we determined the viability of using conditionally immortal cell lines isolated from an H-2kbtsA58 transgenic mouse (Jat et al., 1991; Barber et al., 2000) and NG108-15 cells for heterologous functional expression of ORs, and we also determined the viability of using OSNs for homologous functional expression. For developing conditionally immortal cell lines, we attempted to isolate immature-OSN-like cells from the olfactory epithelium of the transgenic mice, but we could not identify any cells that promoted the functional expression of a target OR without the transfection of RTP expression vectors. The odorant responses of ORs in the NG108-15 cells were weaker, and their lowest responsive concentrations were higher than the corresponding values for the HEK293 cells. In the assessments of homologous expression, we could not find isolated OSNs that expressed the target ORs after electroporation of OR expression vectors into the olfactory epithelium. Therefore, HEK293 cells were used as the functional expression system for ORs.

4. Discussion

4.1. Heterologous functional expression system

We constructed a heterologous functional OR expression system using commercially available HEK293 cells. Zhuang and Matsunami previously reported Ca^{2+} responses of ORs via a chimeric $G\alpha_{15olf47}$ in which the C-terminal 57 amino acids of $G\alpha_{15}$ were replaced by the C-terminal 47 amino acids of $G\alpha_{olf}$, but there was no comparison between responses of $G\alpha_{15olf47}$ and $G\alpha_{15}$ (Zhuang and Matsunami, 2007). In the present study, we constructed another chimeric $G\alpha_{15\_olf}$ in which only the 4 amino acids in the C-terminal region were different from $G\alpha_{15}$. In the HEK293 cells that coexpressed RTPs and the chimeric $G\alpha_{15\_olf}$, ORs showed robust Ca^{2+} responses, good reproducibilities, and relative sensitivities that were similar to the original relative sensitivities of the ORs in isolated OSNs. This OR expression system seems to be the most suitable system for determining the detailed odorant specificities of target ORs by using an SRA analysis of several series of ligands.

4.2. Effect of Gα-binding specificity to ORs on cellular Ca^{2+} responses

The odorant specificity of an OR should be determined on the basis of the binding affinities of ligands to the ligand-binding sites on ORs in an agonistic-interaction manner. In the OSNs, odorant signals activate ORs and are transferred to $G\alpha_{olf}$ and amplified by the cAMP 2nd messenger system via $G\alpha_{olf}$-dependent adenylyl cyclase. In the HEK293 cells that functionally express ORs, coexpression of a specific Gα is required for odor-induced transient Ca^{2+} increases via the IP_3 signal cascade.

After OR activation, several interactions between the IP_3 signal cascade components may affect the sensitivity of cellular Ca^{2+} responses in HEK293 cells. The sequential cascade comprises the following 5 steps: (1) the OR and Gα subunit interact, (2) the Gα subunit and phospholipase C (PLC) interact, (3) IP_3 is generated, (4) IP_3 activates the IP_3-receptor, and (5) the IP_3-receptor mediates Ca^{2+} release from the intracellular Ca^{2+} store. In heterologous functional expression systems, the original binding specificities of Gα in the 1st and 2nd cascade step can be alternatively maintained. We attempted to maintain the original binding specificity of Gα in the 1st step, because it is expected that the specific binding of Gα to ORs should be higher than that of Gα to PLC. The chimeric $G\alpha_{15\_olf}$ improved the response amplitudes, relative sensitivities, and reproducibility of the ORs compared to that constructed using $G\alpha_{15}$. These improvements resulted in high system performance that was sensitive to small differences in Ca^{2+} responses. Although we could not explain all the changes in each cascade step, it is likely that the high binding specificity of Gα contributed to the high sensitivity of Gα to active ORs. Such an OR-sensitive Gα can be readily converted to active Gα by activated ORs in a rapid and stable manner. This process leads to a rapid and stable kinetics of PLC activation and its subsequent deactivation by binding with the active Gα for an adequate period.

In a subpopulation of transfected HEK293 cells, a low binding specificity of $G\alpha_{15}$ to ORs could have resulted in the slow increase in the active $G\alpha_{15}$ concentration. This could have led to a large variation in the initiation time and magnitude of PLC activation and deactivation, thereby causing unstable Ca^{2+} responses. In conclusion, the heterologous OR expression system that coexpresses $G\alpha_{15\_olf}$ and RTPs was suitable for determining the detailed odorant specificities of target ORs.

Authors' contributions

HH and TS planned the experiments. HH performed all Ca-imaging experiments using the functional expression system and constructed all expression vectors used in the final experiment. LS and LB constructed initial versions of some expression vectors and maintained the HEK293 cell line at the beginning of this project. LS also screened conditionally immortalized cells. JH and TS set up the equipment and assayed odorant responses of electroporated OSNs. The manuscript was compiled by HH and TS.

Conflict of interests

The authors declare that there are no competing financial interests.

Acknowledgements

We would like to thank Drs. Kaoru Kato and Toshikazu Majima for kindly providing NG108 cells and bovine serum for the initial testing of the heterologous functional expression system. This study was supported by Grant-in-Aids for Scientific Research (B) #18300066 (TS and JH) and #15360444 (TS) from the MEXT, grants from the MITI, Japan (TS and JH), and JSPS fellowships (HH, LS, and LB) and their Grant-in-Aids from the Japan Society for the Promotion of Science, and a collaborative research fund from the Japan Tobacco Inc.

Appendix A. Supplementary data

Supplementary data associated with this article can be found, in the online version, at doi:10.1016/j.jneumeth.2009.09.024.

References

Abaffy T, Malhotra A, Luetje CW. The molecular basis for ligand specificity in a mouse olfactory receptor. J Biol Chem 2007;282:1216–24.
Abaffy T, Matsunami H, Luetje CW. Functional analysis of a mammalian odorant receptor superfamily. J Neurochem 2006;97:1506–18.
Araneda RC, Peterlin Z, Zhang X, Chesler A, Firestein S. A pharmacological profile of the aldehyde receptor repertoire in rat olfactory epithelium. J Physiol 2004;555:743–56.
Bakalyar HA, Reed RR. Identification of a specialized adenylyl cyclase that may mediate odorant detection. Science 1990;250:1403–6.
Barber RD, Jaworsky DE, Yau KW, Ronnett GV. Isolation and in vitro differentiation: a conditionally immortalized murine olfactory receptor neurons. J Neurosci 2000;20:3695–704.
Buck L, Axel R. A novel multigene family may encode odorant receptors: a molecular basis for odor recognition. Cell 1991;65:175–87.
Carson C, Saleh M, Fung FW, Nicholson DW, Roskams AJ. Axonal dynactin p150^{Glued} transports caspase-8 to drive retrograde olfactory receptor neuron apoptosis. J Neurosci 2005;25:6092–104.
Conklin BR, Herzmark P, Ishida S, V.-Yasenetskaya TA, Sun Y, Farfel Z, Bourne HR. Carboxyl-terminal mutations of $G_{q\alpha}$ and $G_{s\alpha}$ that alter the fidelity of receptor activation. Mol Pharmacol 1996;50:885–90.
Floriano WB, Vaidehi N, Goddard WA, Singer MS, Shepherd GM. Molecular mechanisms underlying differential odor responses of a mouse olfactory receptor. Proc Natl Acad Sci USA 2000;97:10712–6.
Gold GH. Controversial issues in vertebrate olfactory transduction. Annu Rev Physiol 1999;61:857–71.
Hamana H, Hirono J, Kizumi M, Sato T. Sensitivity-dependent hierarchical receptor codes for odors. Chem Senses 2003;28:87–104.
Hirono J, Sato T, Tonoike M, Takebayashi M. Simultaneous recording of $[Ca^{2+}]_i$ increases in isolated olfactory receptor neurons retaining their original spatial relationship in intact tissue. J Neurosci Methods 1992;42:185–94.
Jat PS, Noble MD, Ataliotis P, Tanaka Y, Yannoutsos N, Larsen L, Kioussis D. Direct derivation of conditionally immortal cell lines from an H-2Kb-tsA58 transgenic mouse. Proc Natl Acad Sci USA 1991;88:5096–100.
Jones DT, Reed RR. G_{olf}: an olfactory neuron specific-G protein involved in odorant signal transduction. Science 1989;244:790–5.
Kajiya K, Inaki K, Tanaka M, Haga T, Kataoka H, Touhara K. Molecular basis of odor discrimination: reconstitution of olfactory receptors that recognize overlapping sets of odorants. J Neurosci 2001;21:6018–25.
Katada S, Hirokawa T, Oka Y, Suwa M, Touhara K. Structural basis for a broad but selective ligand spectrum of a mouse olfactory receptor: mapping the odorant binding site. J Neurosci 2005;25:1806–15.
Kleene SJ. Origin of the chloride current in olfactory transduction. Neuron 1993;11:123–32.
Krautwurst D, Yau KW, Reed RR. Identification of ligands for olfactory receptors by functional expression of a receptor library. Cell 1998;95:917–26.
Kurahashi T, Yau KW. Co-existence of cationic and chloride components in odorant-induced current of vertebrate olfactory receptor cells. Nature 1993;363:71–4.
Lancet D. Vertebrate olfactory reception. Annu Rev Neurosci 1986;9:329–55.
Lowe G, Gold GH. Nonlinear amplification by calcium-dependent chloride channels in olfactory receptor cells. Nature 1993;366:283–6.
Malnic B, Hirono J, Sato T, Buck L. Combinatorial receptor codes for odors. Cell 1999;96:713–23.
Mori K, Nagao H, Yoshihara Y. The olfactory bulb: coding and processing of odor molecule information. Science 1999;286:711–5.
Nakamura T, Gold GH. A cyclic nucleotide-gated conductance in olfactory receptor cilia. Nature 1987;325:442–4.
Saito Y, Nothacker H-P, Wang Z, Lin SHS, Leslie F, Civelli O. Molecular characterization of the melanin-concentrating-hormone receptor. Nature 1999;400:265–9.
Saito H, Kubota M, Roberts RW, Chi Q, Matsunami H. RTP family members induce functional expression of mammalian odorant receptors. Cell 2004;119:679–91.
Sato T, Hirono J, Tonoike M, Takebayashi M. Two types of increases in free Ca^{2+} evoked by odor in isolated frog olfactory receptor neurons. Neuroreport 1991;2:229–32.
Sato T. Odorant responsiveness and molecular mechanism of olfactory receptor neuron: As viewed from the dynamical changes in cytoplasmic calcium concentration. Jpn J Taste Smell Res 1994;1:7–16.
Sato T, Hirono J, Tonoike M, Takebayashi M. Tuning specificities to aliphatic odorants in mouse olfactory receptor neurons and their local distribution. J Neurophysiol 1994;72:2980–9.
Shirokova E, Schmiedeberg K, Bedner P, Niessen H, Willecke K, Raguse JD, Meyerhof W, Krautwurst D. Identification of specific ligands for orphan olfactory receptors. J Biol Chem 2005;280:11807–15.
Takeuchi H, Kurahashi T. Mechanism of signal amplification in the olfactory sensory cilia. J Neurosci 2005;25:11084–91.
Touhara K, Sengoku S, Inaki K, Tsuboi A, Hirono J, Sato T, Sakano H, Haga T. Functional identification and reconstitution of an odorant receptor in single olfactory receptor neurons. Proc Natl Acad Sci USA 1999;96:4040–5.
Touhara K. Deorphanizing vertebrate olfactory receptors: recent advances in odorant-response assays. Neurochem Int 2007;51:132–9.
Zhang X, Firestein S. The olfactory receptor gene superfamily of the mouse. Nat Neurosci 2002;5:124–33.
Zhuang H, Matsunami H. Synergism of accessory factors in functional expression of mammalian odorant receptors. J Biol Chem 2007;282:15284–93.
Zufall F, L.-Zufall T, Greer CA. Amplification of odor-induced Ca^{2+} transients by store-operated Ca^{2+} release and its role in olfactory signal transduction. J Neurophysiol 2000;83:501–12.

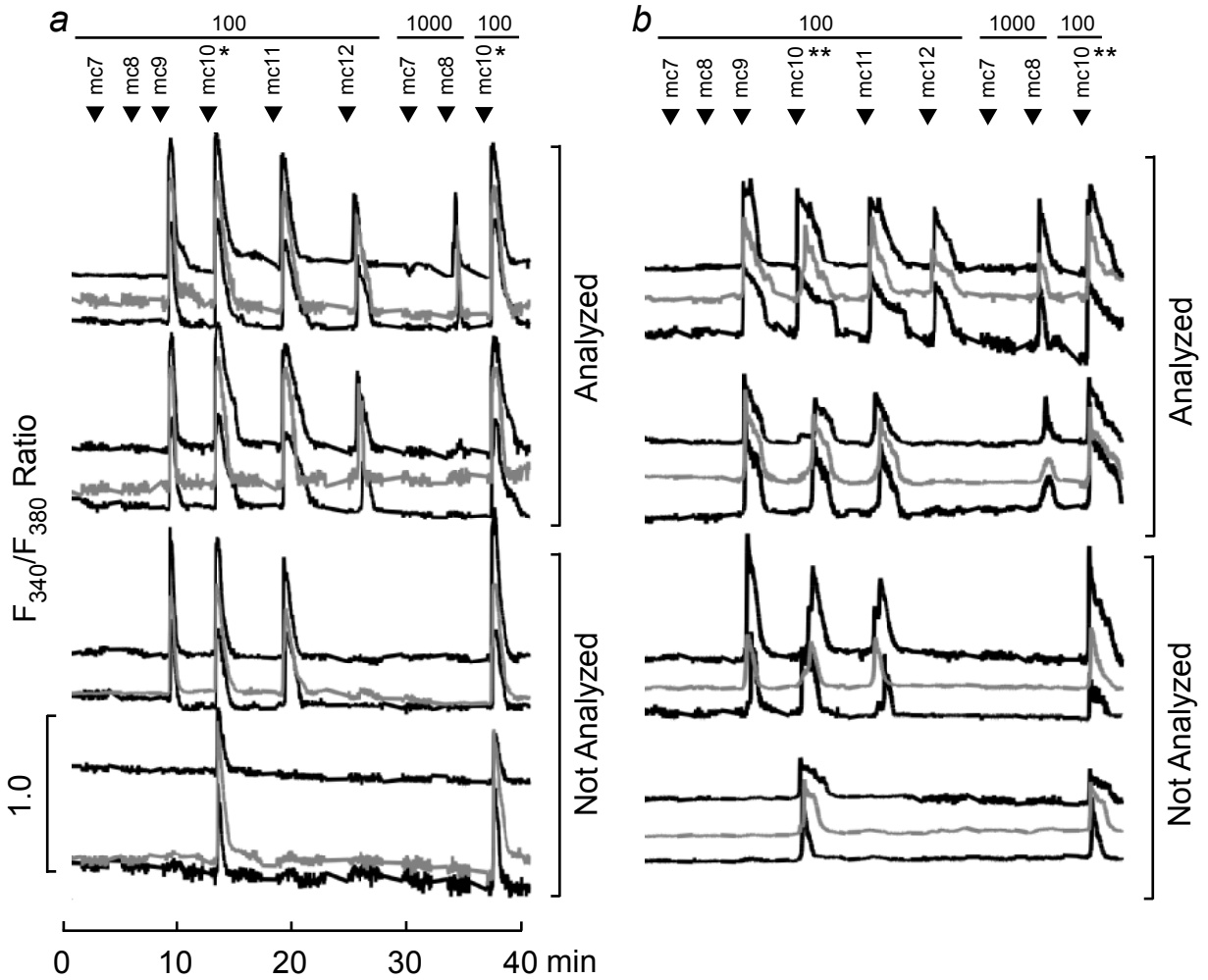

Supplementary Fig. S1. Response curves of single cells for different OR-S83 responsiveness in heterologous expression system coexpressing $G\alpha_{15\_olf}$ or $G\alpha_{15}$. *a*, OR-S83 response curves of 3 HEK293 cells that coexpressed RTP1, RTP2, and $G\alpha_{15\_olf}$ for each of 4 responsiveness types; *b*, OR-S83 response curves of 3 HEK293 cells that coexpressed RTP1, RTP2, and $G\alpha_{15}$ for each of 4 responsiveness types. Responses in the cells that showed 4/5 or higher response rates to responsive ligands were analyzed for response kinetics. Odorant concentrations are shown in μM.

Supplementary Table S1: Differences in OR-S83 response kinetics between $G\alpha_{15\_olf}$ and $G\alpha_{15}$

Agonist	$G\alpha_{15\ olf}$	$G\alpha_{15}$	Significance
Onset latency (s) of Ca^{2+} response			
1 mM mc8	23.8 ± 2.0[†1]	42.3 ± 1.2[†2]	$P < 0.00001$
100 μM mc9	17.7 ± 0.6	21.0 ± 1.0	$P = 0.00581$
100 μM mc10	7.9 ± 0.4	28.8 ± 3.1	$P < 0.00001$
100 μM mc10 (2nd stim.)	6.4 ± 0.4	18.3 ± 1.0	$P < 0.00001$
100 μM mc11	9.9 ± 0.6	25.0 ± 1.3	$P < 0.00001$
100 μM mc12	18.5 ± 2.0	27.7 ± 2.6[†3]	$P = 0.01137$
Latency (s) of peak response			
1 mM mc8	38.6 ± 2.7[†1]	57.3 ± 4.5[†2]	$P = 0.00056$
100 μM mc9	28.7 ± 0.8	37.3 ± 3.3	$P = 0.00627$
100 μM mc10	25.9 ± 1.0	55.8 ± 6.9	$P = 0.00002$
100 μM mc10 (2nd stim.)	24.9 ± 1.1	33.8 ± 2.6	$P = 0.00149$
100 μM mc11	28.1 ± 1.3	42.7 ± 3.7	$P = 0.00018$
100 μM mc12	33.4 ± 2.0	43.3 ± 5.5[†3]	$P = 0.04253$
Peak response amplitude			
1 mM mc8	0.34 ± 0.03	0.17 ± 0.03	$P = 0.00113$
(%Average response)	(145% of 0.231)	(184% of 0.091)	
100 μM mc9	0.74 ± 0.03	0.45 ± 0.05	$P < 0.00001$
(%Average response)	(105% of 0.704)	(126% of 0.359)	
100 μM mc10	0.74 ± 0.03	0.39 ± 0.04	$P < 0.00001$
(%Average response)	(105% of 0.708)	(186% of 0.211)	
100 μM mc10 (2nd stim.)	0.73 ± 0.04	0.47 ± 0.04	$P = 0.00002$
(%Average response)	(106% of 0.693)	(129% of 0.364)	
100 μM mc11	0.63 ± 0.03	0.42 ± 0.03	$P = 0.00002$
(%Average response)	(112% of 0.561)	(167% of 0.253)	
100 μM mc12	0.42 ± 0.03	0.12 ± 0.04	$P < 0.00001$
(%Average response)	(137% of 0.304)	(108% of 0.109)	
Peak width (s) at half-maximum			
1 mM mc8	23.4 ± 3.0[†1]	22.4 ± 3.7[†2]	$P = 0.82193$
100 μM mc9	36.8 ± 2.1	54.8 ± 5.1	$P = 0.00090$
100 μM mc10	54.3 ± 3.2	66.7 ± 7.3	$P = 0.10363$
100 μM mc10 (2nd stim.)	53.2 ± 2.8	63.3 ± 5.6	$P = 0.09123$
100 μM mc11	58.8 ± 4.5	60.6 ± 9.1	$P = 0.85339$
100 μM mc12	47.6 ± 4.7	52.2 ± 10.0[†3]	$P = 0.63924$
Time constant of single-exponential decay for Ca^{2+} recovery			
1 mM mc8	51.3 ± 10.5[†1]	77.6 ± 9.9[†2]	$P = 0.08969$
100 μM mc9	48.6 ± 5.1	113 ± 17	$P = 0.00024$
100 μM mc10	92.1 ± 8.9	174 ± 40	$P = 0.03229$
100 μM mc10 (2nd stim.)	78.7 ± 7.5	189 ± 35	$P = 0.00133$
100 μM mc11	108 ± 12	162 ± 34	$P = 0.11180$
100 μM mc12	133 ± 19	187 ± 48[†3]	$P = 0.21537$

Parameters for Ca^{2+} responses of OR-S83 in the HEK293 cells are shown as mean ± SE. Peak response amplitude is shown as an average of peak response amplitudes and the ratio (%) to the average response is shown in parentheses. An average was calculated for $G\alpha_{15\_olf}$ (n = 29 or 25[†1]) and $G\alpha_{15}$ (n = 23, 17[†2] or 12[†3]). For onset latencies, peak latencies, and peak response amplitudes, all parameters were significantly different between $G\alpha_{15\_olf}$ and $G\alpha_{15}$ ($P < 0.05$)

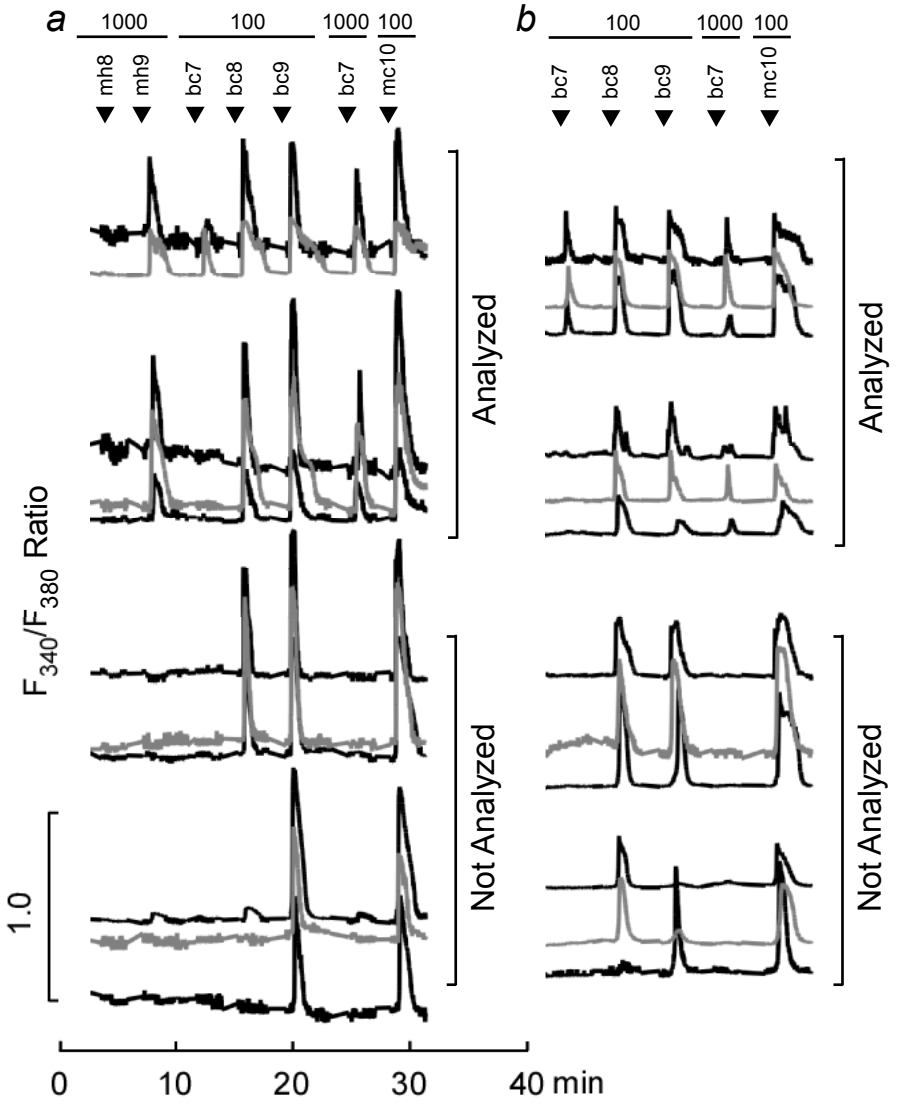

Supplementary Fig. S2. Response curves of single cells for different OR-S83 responsiveness in heterologous expression system coexpressing $G\alpha_{15\_olf}$ or $G\alpha_{15}$. *a*, OR-S83 response curves of 2 or 3 HEK293 cells that coexpressed RTP1, RTP2, and $G\alpha_{15\_olf}$ for each of 4 responsiveness types; *b*, OR-S83 response curves of 3 HEK293 cells that coexpressed RTP1, RTP2, and $G\alpha_{15}$ for each of 4 responsiveness types. Responses in the cells that showed 4/5 or higher response rates to responsive ligands were analyzed for response kinetics. Odorant concentrations are shown in μM.

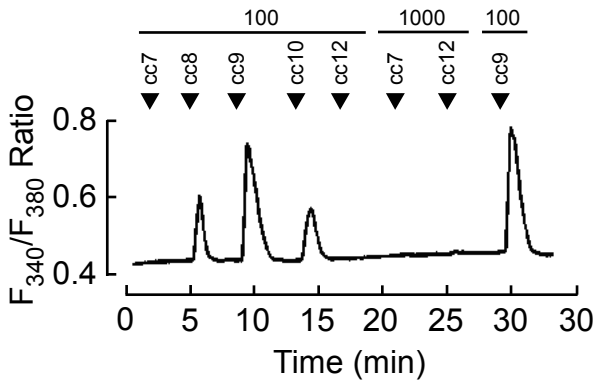

Supplementary Fig. S3. Ca^{2+} response of OR-S6 in HEK293 cells that coexpressed $G\alpha_{15}$.

Ca^{2+} responses of OR-S6 in HEK293 cells that coexpressed $G\alpha_{15}$ for cc-series compounds are demonstrated. The most potent agonist was cc9 as shown in other systems but relative response amplitudes for cc8 and cc10 were somewhat different from those that coexpressed $G\alpha_{15\_olf}$.